stellarator news

**Published by Fusion Energy Division, Oak Ridge National Laboratory**
**Building 9201-2 P.O. Box 2009 Oak Ridge, TN 37831-8071, USA**

Editor: James A. Rome Issue 80 March 2002
E-Mail: jar@ornl.gov Phone (865) 574-1306
On the Web at *http://www.ornl.gov/fed/stelnews*

# Highlights of the 13th International Stellarator Workshop

The 13th International Stellarator Workshop was held at the Australian National University in Canberra, Australia, from 25 February through 1 March 2002. Nearly 100 scientists from around the world attended.

In what follows, I present some of the highlights. My selection and interpretation are inevitably subjective and incomplete, and interested readers can peruse the papers that were presented on the Workshop Web site at

http://wwwrsphysse.anu.edu.au/admin/stellarator/draftproc.html

- Results from the larger devices [Large Helical Device (LHD), Wendelstein 7-AS (W7AS), Compact Helical System (CHS), Heliotron-J)] showed confinement of multi-keV plasmas produced with a variety of heating schemes [electron cyclotron heating (ECH), neutral beam injection (NBI), ion cyclotron radio frequency (ICRF)]. Generation of large radial electric fields is common in these discharges. Key questions for the future are whether even larger electric fields can further improve hot ion confinement, and how these effects compare with confinement in optimized magnetic configurations, e.g., those with orbit optimization due to the design of their modular coils, or those in which auxiliary magnetic fields are used to improve orbit confinement.
- Results from LHD show that discharges with megawatt heating can be maintained for periods of minutes.
- Experiments on W7AS have demonstrated the feasibility of electron-Bernstein wave heating at high electron densities.
- In W7AS, local helical divertors have been shown to be effective in obtaining high-density discharges with low core radiation losses and without impurity accumulation. These results are compatible with the results of modeling studies.
- On LHD, the local island divertor coil system has been successfully used to study island formation and healing in finite-pressure discharges.
- Confinement studies over a wide range of rotational transform profiles with $\iota/(2\pi) > 1$ in the TJ-II heliac show that when the effect of low-order resonances is excluded, confinement is close to that predicted from ISS-95 scaling with a transform dependence ~ $[\iota/(2\pi)]^{0.4}$.

## *In this issue . . .*

- High-beta experiments on W7AS, LHD, and CHS show stable confinement of plasmas with plasma pressure $\beta$ = 2–3%. Some MHD oscillations (probably interchanges) are observed, but these appear to have little or no effect on confinement. There is also some evidence of beta self-stabilization. In the light of these results, theoretical predictions of pressure limits seem more like guidelines than hard limits. However, ballooning instabilities in three-dimensional (3-D) stellarator geometries are quite complex and require considerable further study in both theory and experiment. Alfvén modes remain a concern for fusion-grade plasmas with hot particle populations. Present experiments on W7AS and future work at Auburn will provide guidance on achieving stable operation in current-carrying stellarators (e.g., low-$R/a$ quasi-symmetric designs).
- There is renewed activity in developing and refining stability theory (magnetohydrodynamics, ion temperature gradient, etc.) in 3-D systems, with increasing attention to the details of actual experiments. In the case of ballooning modes, toroidal localization within field periods is an important feature of several theoretical treatments.
- The generation and effects of radial electric fields $E_r$ has become an important area of investigation in its own right—it figures in about a quarter of the papers presented at the workshop. The presence of resonances in transform and turbulence can significantly change $E_r$ from its neoclassically predicted values. Increasing $E_r$ to higher values using techniques such as particle loss driven by perpendicular NBI provides a possible route to increasing ion temperatures in present-generation devices.
- Experiments on a number of devices (TJ-II, CHS, H-1, W7AS, LHD, and others) show that turbulence, transport, and confinement transitions are intimately linked. Results from H-1 show the effects of non-ambipolarity and zonal flows on turbulence levels and transport.
- Low-order resonances are frequently a nuisance in experiments, but they have also found a role as tools for $E_r$ modification, transport barrier formation, and the formation of divertor topologies.
- Theory and configuration design efforts are aggressively exploiting quasi-symmetry in the synthesis of new configurations [W7X, National Compact Stellarator Experiment (NCSX), Quasi-Poloidal Stellarator (QPS), CHS-QA, Heliotron-J, etc.]. Extensive numerical optimization of transport, equilibrium, stability, and engineering properties is now a standard feature of these design activities.
- While notable progress has been made in stellarator research overall, the world stellarator program faces important challenges in the coming years. Lead times for the construction of the next generation of devices are ~5 years, which makes maintaining continuity in research programs more difficult. The development of a compelling reactor vision based on the stellarator is an important task, especially in the context of renewed activity on the ITER tokamak project. The sharing of ideas, techniques, and results via international collaboration is more important than ever.

Jeffrey H. Harris
Australian National University

E-mail: Jeffrey.Harris@anu.edu.au
Phone: +61 6 249 5422

## NCSX in 2003 budget proposal

Plans to design and construct a new stellarator, the National Compact Stellarator Experiment (NCSX), are highlighted in the U.S. Fusion Energy Sciences budget submission to the U.S. Congress for Fiscal Year 2003. The budget includes $11 million to initiate the project.

In undertaking this new initiative, the U.S. Department of Energy's Office of Science cited the opportunities to advance fusion science and to improve the vision of fusion energy. The flexibility to control the three-dimensional (3-D) plasma shape, internal and external sources of rotational transform, and helical ripple provides the program with unique capabilities for understanding toroidal physics. The quasi-axisymmetric NCSX uses 3-D plasma shaping and stellarator fields to produce a stable high-beta configuration that could have transport properties similar to those of tokamaks. The compact stellarator offers the possibility of an improved magnetic confinement system, one that would operate steady-state with no disruptions, no recirculating power for current drive or feedback control, and tokamak-like power density.

The NCSX was endorsed as a proof-of-principle experiment in 2001 by the U.S. Fusion Energy Sciences Advisory Committee (FESAC), which stated that its "gains earn for the compact stellarator an important place in the portfolio of confinement concepts being pursued by the U.S. Fusion Energy Sciences program." The national NCSX team is led by a partnership between the Princeton Plasma Physics Laboratory and the Oak Ridge National Laboratory.

G. H. Neilson
Princeton Plasma Physics Laboratory
Princeton, NJ 08544, USA

E-mail: HNeilson@pppl.gov

# Recent Progress in the LHD Experiment

The Large Helical Device (LHD) is a large heliotron-type device, the world's largest superconducting fusion device. The principal goal of the LHD experiment is to demonstrate high performance of helical plasmas in a reactor-relevant plasma regime. In the first four years of the experiment, we have made good progress in achieving high-quality plasmas. The plasma parameters achieved so far are listed in Table I. Recently a central electron temperature of 10 keV has been obtained by localizing electron cyclotron resonance (ECR) power deposition (a total of 1.2 MW) within $\rho = 0.2$.

**Table 1.** LHD plasma parameters

| | $T$ | $n_e$ |
|---|---|---|
| High Electron Temperature | 10 keV | $6.0 \times 10^{18}$ m$^{-3}$ |
| High Ion Temperature | 5 keV | $8.0 \times 10^{18}$ m$^{-3}$ |
| High Confinement | 1.1 keV | $6.5 \times 10^{19}$ m$^{-3}$ |
| $\tau_E$ = 0.3 s, $nT\tau_e = 2.1 \times 10^{19}$ keV m$^{-3}$, $P_{abs}$ = 2 MW, | | |
| Maximum Stored Energy | $W_p$ = 1.16 MJ | |
| Highest Beta | $\langle\beta\rangle \sim 3.2\%$ at $B$ = 0.5 T | |
| Maximum Density | $1.5 \times 10^{20}$ m$^{-3}$ | |

## Global energy confinement

The energy confinement times $\tau_E$ in the LHD inward-shifted configuration ($R_{ax}$ = 3.6 m) are consistent with the ISS95 scaling with an enhancement factor of ~1.5 and are comparable to those in ELMy H-mode discharges (tokamaks). They are a factor of 2 higher than those of smaller heliotron devices such as the Compact Helical System (CHS), Heliotron-E, and the Advanced Toroidal Facility (ATF). This enhancement is attributed to high edge temperature. The enhancement factor over the ISS95 scaling is found to be sensitive to variation in the location of the magnetic axis $R_{ax}$ as shown in Fig. 1. It is optimum at $R_{ax}$ = 3.55–3.6 m and decreases with increasing $R_{ax}$. For $R_{ax}$ = 3.9 m, it is as small as 0.6. Furthermore, deterioration of the confinement occurs for $R_{ax}$ = 3.75 and 3.9 m when the plasma becomes collisionless ($\nu^* < 1$). This appears to be due to neoclassical transport. For inward-shifted discharges with good particle orbit properties and hence low neoclassical transport, the enhancement factor is independent of $\nu^*$ and hence the anomalous transport dominates the neoclassical transport.

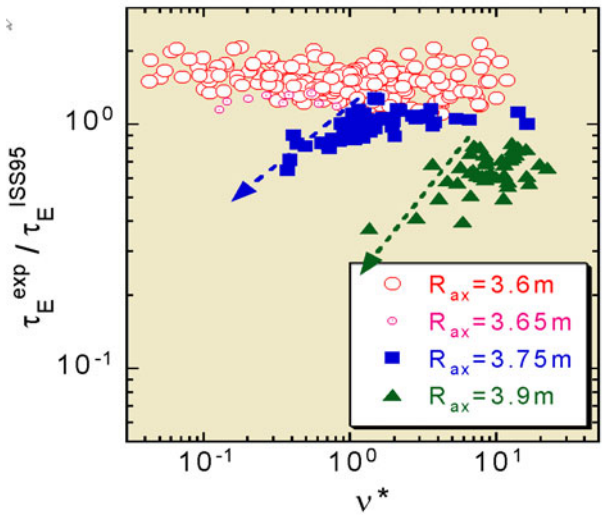


**Fig. 1.** Enhancement factor over ISS95 as a function of $\nu^*$ for various configurations ($R_{ax}$)

## High edge temperature

The temperature profiles in the LHD discharges are very broad with high edge temperature. A mild discontinuity in $\nabla T_e$ often appears around $\rho = 0.85$ (where $\iota/(2\pi)$ is unity); it is probably caused by some mechanisms involving islands. When an error field ($n/m$ = 1/1) is minimized by external perturbation coils, the island effect almost disappears and the profile becomes close to parabolic [see Fig. 2 (top)] for a wide range of the plasma parameters. The LHD density profile is generally very flat. A high density gradient exists in the ergodic region, just outside of the last closed flux surface (LCFS) at $\rho = 1$ where the electron temperature is kept low by high electron parallel heat transport. The gradient is not surprising since cold ions are well confined in the open edge region, where the connection length is longer than 300 m. This situation is quite a contrast to the tokamak H-mode discharges, which are characterized by a very sharp density gradient just inside the LCFS. The broad temperature profile always appears whenever appreciable power reaches the divertor plates.

Considering these observations, the present LHD discharges, which exhibit a factor of 1.5 enhancement, are not H-mode discharges. The edge temperature and density (at $\rho = 0.9$), however, are comparable to those of the comparable H-mode tokamaks, but the edge pressure gradient is much milder. The edge pressure gradient is not limited by an MHD instability as in tokamaks. For high-beta dis-

charges ($\beta$ = 2–3%), the normalized pressure gradient $d\beta/d\rho$ becomes as high as 0.07 at the middle of the steep gradient; this exceeds the Mercier stability limit. The relatively high edge temperature gradient leads to a transition from the ion root (negative radial electric field) to electron root (positive $E_r$) for the low-density discharges ($n < 1\times10^{19}$ m$^{-3}$). This transition, however, has not resulted in reduction of the edge anomalous thermal diffusivity.

## Internal transport barrier

Enhancement of confinement is a major research goal of the LHD program. As discussed above, the temperature profile in the normal LHD discharge is close to parabolic. However, when the ECR heating (ECRH) power is absorbed in the central region ($\rho < 0.2$) of the discharges heated with counter-injected neutral beams, an internal transport barrier (ITB) appears, as shown in Fig. 2. This

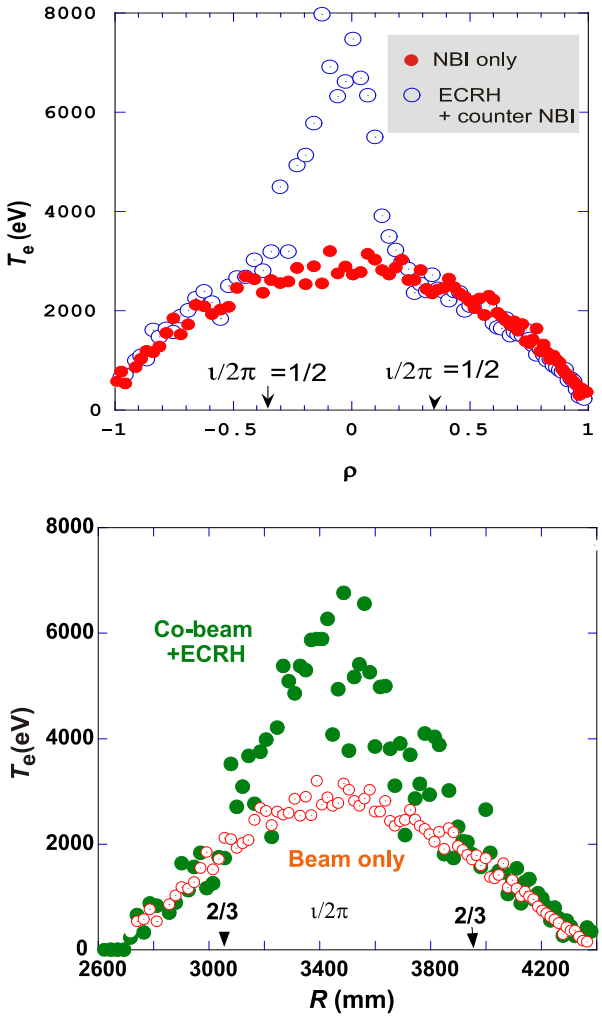


**Fig. 2**. Profiles of $T_e$ for discharges with NBI only and with NBI and ECRH. The profiles are broad with NBI only, but an ITB forms when ECH is added to both counter- (top) and co-injected (bottom) discharges. In both cases, $B$ = 2.84 T, $R_{ax}$ = 3.5 m, $n = 6\times10^{18}$ m$^{-3}$.

ITB profile is obtained when the ECRH power exceeds a threshold value. This threshold increases with increasing density and decreasing NBI power. The location of the "foot" of the ITB, i.e., the discontinuity in $\nabla T_e$, is found to be near the $\iota/(2\pi) = 0.5$ surface. In the ITB region, the positive electric field is seen, indicating its role in formation of the ITB. For discharges with 1 MW of co-injected NBI heating and ECRH (Fig. 2 bottom), on the other hand, a broader ITB appears and the foot location is around $\iota/(2\pi) = 2/3$. In the ITB region, the power flux originating from NBI, which has a broad power deposition, is much less than that from centrally focused ECR power. But the direction of the beam strongly influences the shape of the $T_e$ profile. One working hypothesis is that the iota profile is modified by beam-driven current. Even though enhancement of the global energy confinement is not observed because of core localization of the improvement, we believe that this is an encouraging sign of global confinement enhancement.

## MHD stability

We achieved average beta $\langle\beta\rangle$ of 3.2% at $B$ = 0.5 T. The maximum $\langle\beta\rangle$, which is limited by the available heating power, is achieved in the inward-shifted configuration ($R_{ax}$ ~ 3.60 m), in which a magnetic hill exists in the entire region. In these discharges, the pressure profile is nearly flat in the core and a high pressure gradient exists in the edge. The observed pressure gradient ($d\beta/d\rho$) exceeds the Mercier stability limit in nearly half of the plasma confinement region. As shown in Fig. 3, it becomes Mercier unstable at $\rho = 0.9$ ($\iota/(2\pi) = 1$) when $\langle\beta\rangle$ exceeds 1.8% and is even unstable to low-$n$ modes theoretically when $\langle\beta\rangle$ exceeds 2.1%. On the other hand, at $\rho = 0.5$ ($\iota/(2\pi) = 0.5$), the observed pressure profile is unstable up to $\langle\beta\rangle$ = 2%, but it becomes stable when $\langle\beta\rangle$ increases fur-

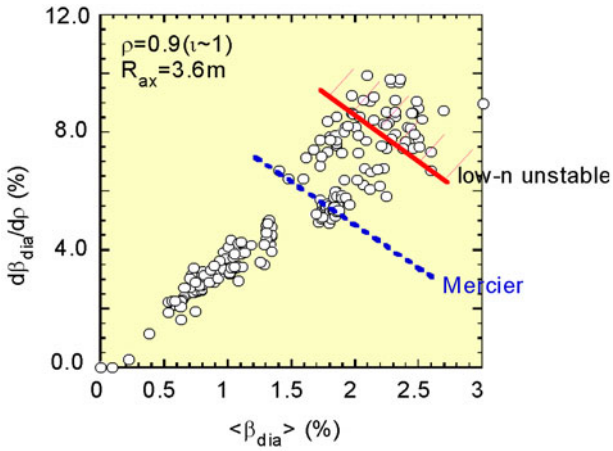


**Fig. 3.** Unstable regimes of edge MHD modes which resonate with $\iota/(2\pi) = 1$ surface in the parameter space ($d\beta/d\rho$, $\beta$). The observed data points are also shown for comparison.

ther. The observed magnetic fluctuations, which generally increase with $\langle\beta\rangle$, do not lead to any serious MHD phenomenon that degrades the confinement time.

It is significant and very encouraging that MHD stability is demonstrated in the inward-shifted configuration, which has good transport properties.

## Island suppression

In toroidal systems, the formation of islands is a major concern because they degrade the confinement and sometimes lead to a disruption. We find that finite-beta collisionless plasmas significantly reduce the size of externally imposed islands. In our experiment, a vacuum island (island without plasma) is generated mainly by a perturbation field produced by a set of external coils and partly by error fields. The parameter space for the island suppression for a case with $R_{ax}$ = 3.6 m, $B$ = 2.8 T, and with $w_{ex}$ = 0.085 (where $w_{ex}$ is the vacuum island full width in terms of ρ) is shown in Fig. 4. We believe that temperature and density at the $\iota/(2\pi)$ =1 surface are important parameters for the island suppression mechanism. The open circles (o) correspond to the cases with undetected islands (which means that $w < 0.5\ w_{ex}$) and the closed circles (•) correspond to those exhibiting a clear island with $w \approx w_{ex}$). Suppression of the island occurs in the higher electron temperature and lower density region (region II).

Instead of electron temperature and density, it may be more appropriate to use the dimensionless quantities beta and $\nu^*$ [$= \nu_\varepsilon(2\pi/\iota)(R/v_e^{th})(Z_{eff}/\varepsilon^{3/2})$ ] at $\iota/(2\pi)$ =1. The parameter space for suppression of the island is $\nu^* < 1.7$ and $\beta > 0.09\%$ (region II). In the low-beta plasma (regions I, IV), the island sizes are found to be close to those of the vacuum island, as expected. Data obtained so far show that the collisionless ($\nu^* < 1$) and finite-beta

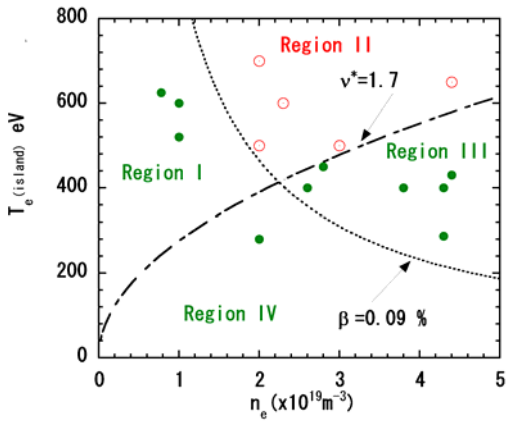


**Fig. 4.** Parameter space ($T_e$(island), $n$) for island suppression for the case $w_{ex}$ = +0.085, $B$ = 2.5–2.75 T, $R_{ax}$ = 3.6 m. o : no island, • : island with $w \sim w_{ex}$. Island suppression occurs in region II.

(> 0.1%) plasma suppresses the island, hopefully leading to stabilization of the most unstable mode ($n/m$ = 1/1), which is predicted to appear at high beta. On the other hand, a significant enlargement of the island ($w \geq 2w_{ex}$) occurs when the plasma parameter is located to the far right in region III (i.e., collisional finite-beta plasma). But this enlargement can be avoided by making the vacuum island small.

## ICRF heating

High-power ion cyclotron range of frequencies (ICRF) heating was carried out and remarkable experimental results were obtained. The optimum heating condition was obtained when the ion cyclotron resonance layer was located at the saddle point of the magnetic field in the minority heating of He majority plasmas with hydrogen minority; i.e., $f$ = 38.47 MHz, magnetic axis $R_{ax}$ = 3.6 m, and $B$ = 2.75 T. Most of the ICRF heating power was absorbed by high-energy hydrogen ions. Results in the ICRF-heated plasma may be summarized as follows:

1. ICRF-sustained mode of operation: the plasma was sustained in the range of $P_{ICRF}$ = 0.2–2.5 MW. The plasma parameters were the average electron density of $n = (0.3 - 2.7) \times 10^{19}$ m$^{-3}$, plasma energy $W_p$ = 30–240 kJ, and temperature $T_e \sim T_i$ = 0.5–2.0 keV.
2. Additional heating of the NBI-heated plasma: The increase in the plasma stored energy during ICRF heating was observed to obey the power scaling of ISS95.
3. Second-harmonic heating was carried out at $B$ = 1.3–1.55 T. The increase in the plasma stored energy was observed at the plasma beta of β = 1%. The heating efficiency increased with the plasma beta.
4. High-energy hydrogen ions were detected up to 250–500 keV. The observed tail temperature was close to the effective temperature deduced from the Stix formula.

## Divertor

The LHD is equipped with an open helical divertor configuration and is normally operated using the divertor. We can also operate with limiter discharges. Limiter operation suffers from radiation problems due to higher impurity concentrations. In 1999 carbon tiles were installed as divertor plates, resulting in a significant reduction in metal impurity (Fe). Since the LHD divertor magnetic configuration has a three-dimensional structure, the divertor/ scrape-off-layer (SOL) structure is not a simple layer as in a tokamak. Numerical field line tracing predicts that split layers with a gap of a few centimeters strike the divertor plates at some locations. Our probe measurement confirms such a structure.

The divertor temperature ($T_{e\,div}$) and density ($n_{div}$) measured by probes on the divertor plates were typically 5–

40 eV and $(0.1 - 5.0) \times 10^{18}$ m$^{-3}$, respectively. In Fig. 5, they are shown with the temperature and density at the last closed flux surface (LCFS) ($n_{\mathrm{LCFS}}$, $T_{\mathrm{e\,LCFS}}$) as a function of the average density. The data are taken from two discharges with different input power ($P_{\mathrm{abs}}$) in which the density is ramped up with time. The electron density at the LCFS is about half the average density $n_{\mathrm{e}}$, while the electron density at the divertor is 1/20–1/30 of $n_{\mathrm{e}}$. These linear relations are insensitive to variation in the input power. The electron temperatures at the LCFS and divertor ($T_{\mathrm{e\,LCFS}}$, $T_{\mathrm{e\,div}}$) decrease gradually with $n_{\mathrm{e}}$. The ratio of $T_{\mathrm{e\,div}}$ to $T_{\mathrm{e\,LCFS}}$ is approximately 0.2 and almost independent of the plasma conditions ($P_{\mathrm{abs}}$, $n_{\mathrm{e}}$). We also find that the temperature ratio remains almost unchanged when the absolute value of the temperature is increased at higher power.

In discharge with low $P_{\mathrm{abs}}$, $T_{\mathrm{e\,LCFS}}$ and $T_{\mathrm{e\,div}}$ decrease gradually with increasing $n_{\mathrm{e}}$ up to $n_{\mathrm{e}} = 3.6 \times 10^{19}$ m$^{-3}$. At this density, the radiative power suddenly increases and both temperatures dramatically drop. There is no sign of a high recycling divertor plasma or a stable detached divertor plasma, which are often observed in tokamaks.

The density limit for LHD discharges increases with increasing heating power and is a factor of 1.5 higher than that predicted by the Sudo empirical scaling [$n_{\mathrm{c}} = 0.25(PB/Ra^2)^{1/2}$]. Here $n_{\mathrm{c}}$ is the averaged electron density ($10^{20}$ m$^{-3}$), $P$ the absorbed power (MW), $B$ the magnetic field strength (T), and $R$ and $a$ are the major and minor radii (m). Density up to $1.5 \times 10^{20}$ m$^{-3}$ has been achieved with pellet injection for a heating power of 8 MW, while a value of $1.2 \times 10^{20}$ m$^{-3}$ has been achieved with gas puffing alone and 5 MW of heating power.

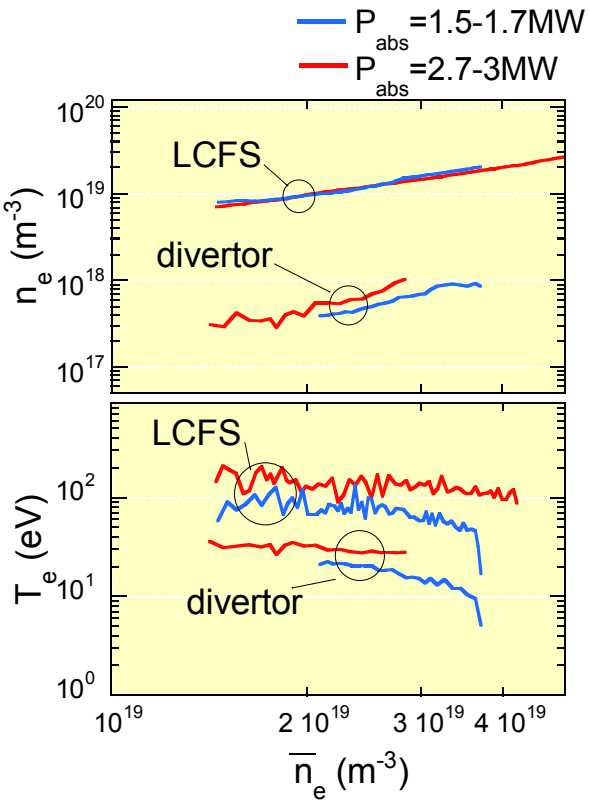


**Fig. 5.** Temperatures and densities at the LCFS and divertor plate are plotted as a function of the average density.

## Long-pulse discharges

Demonstration of a steady-state plasma with high performance is one of the most challenging issues. Such investigation is particularly appropriate for the LHD program. An ICRF-heated plasma (0.4 MW) with a discharge duration of 2 minutes was achieved. In this discharge with helium gas, the electron densities are maintained around $1 \times 10^{19}$ m$^{-3}$ and the temperatures are > 1 keV. The radiated power is less than 25% of the input power, and there is no sign of impurity accumulation. As to the operational density limit in long-pulse discharges, a high-density plasma with $6.7 \times 10^{19}$ m$^{-3}$ was sustained for 10 s with NBI power of 2 MW. The global energy confinement of long-duration plasmas is almost the same as that in short-pulse discharges.


N. Ohyabu, A. Komori, K. Kawahata, O. Kaneko, H. Yamada, Y. Nakamura, K. Ida, T. Akiyama,[1] N. Ashikawa,[2] M. Emoto, H. Funaba, P. Goncharov,[2] M. Goto,H. Idei, K. Ikeda, S. Inagaki, M. Isobe, H. Kawazome,[3] K. Khlopenkov, T. Kobuchi, A.Kostriookov,S. Kubo, R. Kumazawa, Y. Liang S. Masuzaki, T. Minami, J. Miyazawa, T. Morisaki, S. Morita, S. Murakami, S. Muto, T. Mutoh, Y. Nagayama, H. Nakanishi, K. Narihara, Y. Narushima, K. Nishimura, N. Noda, T. Notake,[4] H. Nozato,[5] S. Ohdachi, Y. Oka, M. Osakabe, T. Ozaki, B. J. Peterson, A. Sagara, T. Saida,[2] K. Saito,[4] S. Sakakibara, R. Sakamoto, M. Sasao K. Sato, M. Sato, T. Seki, T. Shimozuma, M. Shoji, H. Suzuki, Y. Takeiri,N., Takeuchi,[4] N. Tamura,[2] K. Tanaka, T. Toi, T. Tokuzawa, Y. Torii,[4] K. Tsumori, K. Y. Watanabe, T. Watari, Y. Xu, I. Yamada,S. Yamamoto,[4] T. Yamamoto,[4] M. Yokoyama, Y. Yoshimura, M. Yoshinuma, K. Itoh,

K. Ohkubo, S. Sudo, K. Yamazaki, O.Motojima, Y. Hamada, M. Fujiwara.

National Institute for Fusion Science, Toki, Gifu 509-5292, Japan

[1] Research Laboratory for Nuclear Reactors, Tokyo Institute of Technology, Tokyo 152-8550, Japan

[2] Department of Fusion Science, School of Mathematical and Physical Science, Graduate University for Advanced Studies, Hayama, 240-0193, Japan

[3] Graduate School of Energy Science, Kyoto University, Uji 611-0011, Japan

[4] Department of Energy Engineering and Science, Nagoya University, 464-8603 Japan

[5] Graduate School of Frontier Sciences, the University of Tokyo 113-0033, Japan